J. Fluid Mech. (1993), vol. 248, pp. 531–541

A note on the distortion of a flat-plate boundary layer by free-stream vorticity normal to the plate

By M. E. GOLDSTEIN[1] AND S. J. LEIB[2]

[1] National Aeronautics and Space Administration, Lewis Research Center, Cleveland, OH 44135, USA

[2] Sverdrup Technology, Inc. Lewis Research Center Group, Cleveland, OH 44135, USA

(Received 28 April 1992 and in revised form 14 October 1992)

The purpose of this note is to construct a local solution that eliminates a residual velocity discontinuity in the inviscid portion of a solution obtained in a recent paper by Goldstein, Leib & Cowley (1992). This result is of importance because it shows that the solution obtained in that paper is entirely non-singular outside the viscous wall boundary layer and that any singularity in the problem will have to arise in the usual way through a breakdown in the viscous boundary layer.

1. Introduction

In a recent paper, Goldstein, Leib & Cowley (1992, hereafter referred to as GLC), analysed the effect of small free-stream non-uniformity on the flow over a relatively thin flat plate. They showed how small (but steady) spanwise variations in the incident streamwise velocity field ultimately cause the initially thin viscous boundary layer flow over the plate to separate. Inviscid vortex stretching in the main stream causes the separation to develop relatively close to the leading edge and a fairly complete analytical description of the separation structure was then obtained. This separation, which appears to be of the boundary-layer collision type (Stewartson, Cebeci & Chang 1980; Stewartson & Simpson 1982), occurs on a symmetry plane with the wall shear stress vanishing at the separation point.

It was assumed that the characteristic dimension of the rounded leading edge was of the order of the spanwise lengthscale, say λ, of the upstream disturbance field, and that the Reynolds number based on λ, say R_λ, was large. The inviscid flow in the vicinity of the leading edge was determined from linear 'rapid distortion' theory (Hunt & Carruthers 1990; Goldstein 1978). The inviscid crossflow effects produced only a linear perturbation to the boundary-layer flow in the vicinity of the leading edge, but they produced order-one changes in the boundary-layer profiles at large distances downstream.

The linear rapid distortion theory solution broke down at large streamwise distances with the breakdown moving further upstream as the surface of the body is approached. A new nonlinear solution was then obtained in order to describe the external inviscid flow in the physically interesting region where order-one changes occur in the boundary-layer profiles. The thickness of this nonlinear region was small compared to its streamwise dimension but large compared to the boundary-layer thickness. It served as kind of a 'blending layer' that connects the boundary-layer solution to the linear rapid distortion theory solution which applies at an order-one (on the scale λ) distance from the wall. This region, in which the horizontal pressure gradients are negligible, might be characterized as a nonlinear vorticity layer.

The blending layer (or nonlinear vorticity layer) flow is governed by the inviscid Burgers' equation (sometimes called the kinematic wave equation) and eventually develops an infinite singularity in the vertical velocity at a certain spanwise location at a finite downstream position owing to the well-known wave steepening effects associated with the solution to that equation. This singularity lies along a curved line (or a periodic array of curved lines) with the flow being discontinuous across the planes extending downstream of these lines. (This plane turned out to be a symmetry plane in the specific numerical example worked out in GLC.) A new local solution was worked out in order to eliminate the singularity in the singularity line region. This solution was still inviscid and did not bring in the horizontal pressure gradients. Moreover, like the blending-layer solution itself, it turned out to be discontinuous across the symmetry plane. The purpose of this note is to show that another local solution can be constructed to completely eliminate the velocity discontinuity across the symmetry plane. This solution is still inviscid but now brings in the horizontal pressure gradients. This result shows that the GLC solution is completely non-singular outside the boundary layer and therefore any singularity in the problem must arise through a breakdown of the viscous boundary layer.

In §2 we review the formulation of GLC and set out the notation used. The local asymptotic solution that eliminates the residual singularity in the inviscid solution of GLC is constructed in §3. The note concludes with a discussion of the results in §4.

2. Review of formulation and the inviscid solutions of GLC

As in GLC we are concerned with the incompressible flow over a semi-infinite flat plate of thickness $h^* = O(\lambda)$. The upstream flow field consists of a uniform stream of velocity U_∞ and a small, $O(\epsilon)$, perturbation, say $\epsilon U_\infty u_\infty(z)$, to the streamwise velocity that depends only on the dimensionless spanwise variable z. All lengths are normalized with λ and all velocities with U_∞. The pressure p is normalized with ρU_∞^2 where ρ is the (constant) density. The streamwise coordinate x has its origin at the leading edge of the plate while that of the transverse coordinate y coincides with the flat surface of the plate far downstream. As in GLC the scaling is chosen so that the viscous effects are confined to a surface boundary layer which is predominantly two-dimensional near the forward stagnation point. This requires that the Reynolds number, $R_\lambda = U_\infty \lambda/\nu$, where ν is the kinematic viscosity, satisfy the inequality

$$\ln R_\lambda \ll 1/\epsilon \ll R_\lambda. \tag{2.1}$$

The overall flow configuration is shown in figure 1 which is taken from GLC.

In this paper we only consider the inviscid portion of the flow. The upstream disturbance produces a linear perturbation to the two-dimensional base flow $\{U_0(x,y), V_0(x,y), 0\}$ in the vicinity of the leading edge where $x = O(1)$, so that the relevant solution expands like

$$\boldsymbol{u} = \{U_0, V_0, 0\} + \epsilon\{u_0, v_0, w_0\} + \epsilon^2\{u_1, v_1, w_1\} + \dots, \tag{2.2}$$

$$p = P_0 + \epsilon p_0 + \epsilon^2 p_1 + \dots, \tag{2.3}$$

in this region. The first-order solutions $\{u_0, v_0, w_0\}$ were obtained by application of the generalized rapid distortion theory of Goldstein (1978), which shows that the spanwise velocity has a weak logarithmic singularity at the surface of the plate that can only be eliminated by viscous effects (see also Lighthill 1956). The expansions (2.2) and (2.3) eventually break down far downstream from the leading edge because, as shown in GLC, the terms $\epsilon^2 u_1$ and $\epsilon^2 w_1$ become of the same order as ϵu_0 and ϵw_0,

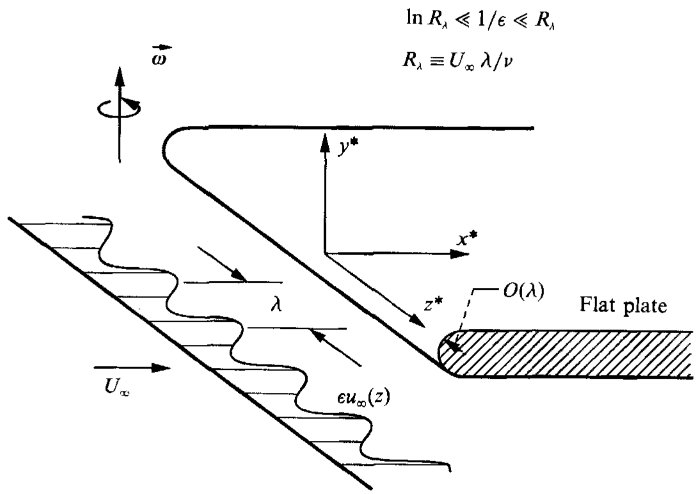

FIGURE 1. Flow configuration.

respectively when $-\epsilon x \ln y = O(1)$. A new solution must therefore be constructed for this region which was called the blending layer by GLC (but might better be referred to as a nonlinear vorticity layer). Within it the scaled variables

$$\bar{x} \equiv \epsilon x/\sigma, \tag{2.4}$$

and

$$\eta \equiv -\sigma \ln y, \tag{2.5}$$

are order one, where

$$\sigma \equiv -1/\ln \delta, \tag{2.6}$$

and $\lambda\delta$ is the thickness of the viscous boundary layer below the blending layer. For convenience

$$\xi \equiv \bar{x}\eta, \tag{2.7}$$

and η are used as independent variables. The relevant solution is of the form

$$u = 1+\epsilon\left[\bar{u}_0(\xi,z)+\sigma\frac{\xi}{\eta}\bar{u}_1(\xi,z)+\ldots\right], \tag{2.8}$$

$$v = \frac{\epsilon}{\sigma}\mathrm{e}^{-\eta/\sigma}[\eta\bar{v}_0(\xi,z)+\sigma\bar{v}_1(\xi,z)+\ldots], \tag{2.9}$$

$$w = \frac{\epsilon}{\sigma}(\eta\bar{w}_0(\xi,z)+\sigma\bar{w}_1(\xi,z)+\ldots], \tag{2.10}$$

$$p = \epsilon^2 d(z)+\frac{1}{2}\left(\frac{\epsilon}{\sigma}\mathrm{e}^{-\eta/\sigma}\right)^2[\eta^2\bar{p}_0(\xi,z)+\sigma\eta\bar{p}_1(\xi,z)+\ldots], \tag{2.11}$$

where $d(z)$ is an arbitrary function of z which comes from the linear rapid distortion theory solution.

The leading-order spanwise velocity $\bar{w}_0$ is governed by the inviscid Burgers' equation, whose solution becomes singular at a finite streamwise position $\xi = \xi_s$, which corresponds to the curve $\xi_s = -\epsilon x \ln y$ shown in figure 2 where the inviscid singularity structure is pictured. Downstream of this curve the spanwise velocity can only be made single valued if it is allowed to be discontinuous across a plane extending downstream of this curve (which in the numerical example of GLC was the

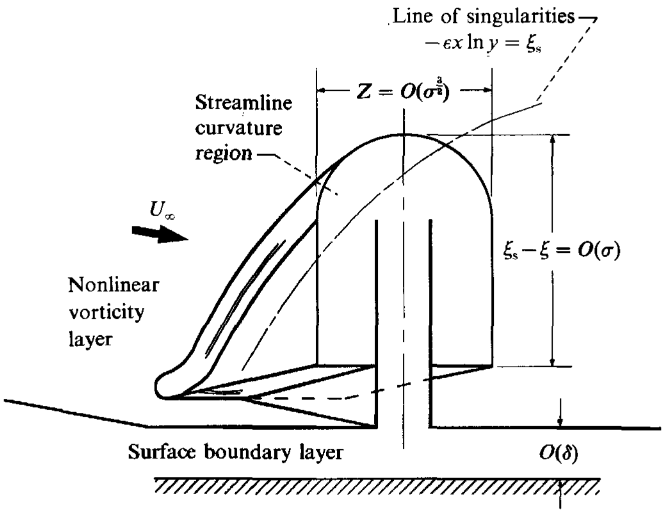

FIGURE 2. Singularity structure of the nonlinear inviscid flow of GLC.

symmetry plane $z = 0$). The breakdown of the inviscid Burgers' equation solution leads to an infinite singularity in the leading-order normal velocity $\bar{v}_0$. A new local solution was constructed by GLC to eliminate this infinite singularity.

In the singularity-line region, where the inner variables

$$\bar{\xi} \equiv \eta(\xi - \xi_s)/\sigma\xi_s - \ln(\xi_s \sigma/\eta) \tag{2.12}$$

and

$$\bar{z} \equiv (\eta/\sigma\beta_s\xi_s)^{\frac{3}{2}} z \tag{2.13}$$

are order one, and β_s is a constant that is fixed by the form of the upstream distortion (see (4.7) of GLC), the solution is of the form

$$u = 1 + O(\epsilon), \tag{2.14}$$

$$v = \frac{\epsilon}{\sigma^2 \xi_s} e^{-\eta/\sigma} \eta^2 \bar{v}_I(\bar{\xi}, \bar{z}) + \dots, \tag{2.15}$$

$$w = \epsilon \left(\frac{\xi_s \beta_s^3 \eta}{\sigma} \right)^{\frac{1}{2}} \bar{w}_I(\bar{\xi}, \bar{z}) + \dots, \tag{2.16}$$

$$p = \epsilon^2 d(0) + \frac{1}{2} \left(\frac{\epsilon \eta^2}{\sigma^2 \xi_s} e^{-\eta/\sigma} \right)^2 \bar{p}_I(\bar{\xi}, \bar{z}) + \dots. \tag{2.17}$$

The local normal velocity $\bar{v}_I$ is now finite but the associated spanwise velocity $\bar{w}_I$ remains discontinuous across $\bar{z} = 0$. The relevant composite solution for these two nonlinear inviscid regions is therefore also bounded but is still discontinuous across an appropriate plane extending downstream from the initial singularity line (which, as in the numerical example of GLC, is taken to be the symmetry plane $z = 0$).

3. Elimination of the spanwise velocity discontinuity

In this section we construct the local asymptotic solution that eliminates the spanwise velocity discontinuity across the $z = 0$ symmetry plane in the blending-layer and singularity-line solutions of GLC. This discontinuity exists both within and

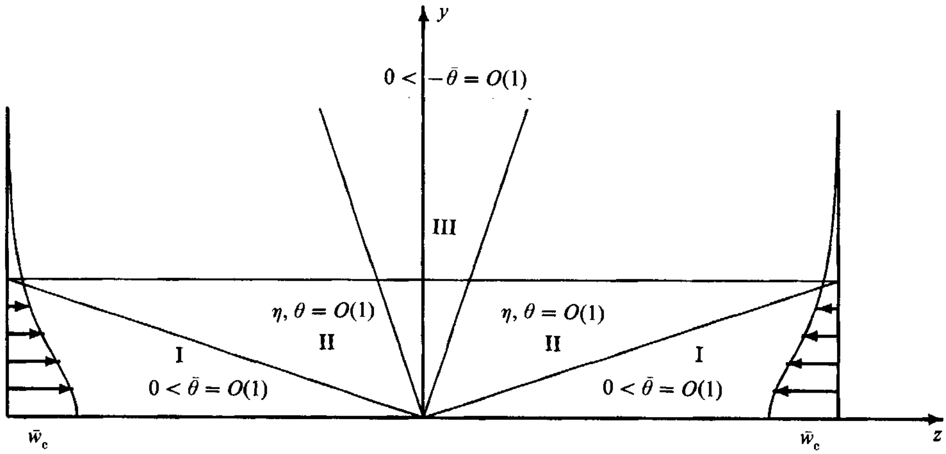

FIGURE 3. Asymptotic structure of the inviscid solution constructed to eliminate the residual velocity discontinuity in the solution of GLC.

downstream of the singularity-line region and it is expedient to deal with both these regions simultaneously. We therefore form a composite solution, say $w_c(\bar{x}, \eta, z)$, using the blending-layer solution (2.10), the singularity line solution (2.16) and its outer limit given by equation (4.30) of GLC as

$$w_c(\bar{x}, \eta, 0^{\pm}) = \pm \frac{\epsilon}{\sigma} \bar{w}_c(\bar{x}, \eta), \tag{3.1}$$

where
$$\bar{w}_c(\bar{x}, \eta) \equiv -\eta \bar{w}_0(\bar{x}\eta, 0^+) \frac{\bar{w}_1(\bar{\xi}, 0^+)}{\bar{\xi}^{\frac{1}{2}}}. \tag{3.2}$$

This result is limited to the case, corresponding to the numerical example of GLC, where w has odd symmetry about $z = 0$. Here $0^{\pm}$ denotes the limiting values as $z \to 0$ through positive/negative z and we have taken $\mu \equiv 0$ in the singularity-line region solution (4.28) of GLC. The composite solution (3.1) and (3.2) is uniformly valid in both the singularity-line region and the downstream blending-layer region. It therefore reduces to the blending-layer solution when $(\xi - \xi_s) = O(1)$ (from (4.30) of GLC) and the singularity-line solution when $\bar{\xi} = O(1)$ (from (4.5)–(4.9) of GLC). Figure 2, along with (2.4), (2.5) and (2.6), shows that the height of the velocity discontinuity is $O(\lambda \delta^{(\xi_s/\bar{x})})$ and is very small compared to the spanwise lengthscales, λ and $\lambda \sigma^{\frac{3}{2}}$, of the blending-layer and singularity-line region solutions, respectively. We can therefore find a region where λz is small compared to λ but still large compared to the height $\lambda \delta^{(\xi_s/\bar{x})}$ of the symmetry plane velocity discontinuity. The spanwise flow entering this region will be given by $w_c(\bar{x}, \eta, 0^{\pm})$ at large values of the appropriately scaled spanwise variable as illustrated in figure 3.

The transverse variations of the flow in this region will, of course, be much more rapid than those in the blending layer and singularity line region and the streamwise, or $\bar{x}$, variations (which just balance the transverse variations in these regions) will, therefore, be negligible there. The relevant flow will then be governed by the two-dimensional vorticity equation, which can be integrated in the usual way to show that the relevant two-dimensional streamfunction ψ:

$$w = \partial \psi / \partial y, \tag{3.3}$$

$$v = -\partial \psi / \partial z, \tag{3.4}$$

satisfies
$$\nabla_T^2 \psi = \tfrac{1}{2}H'(\psi), \tag{3.5}$$
where ∇_T^2 denotes the transverse Laplacian
$$\nabla_T^2 \equiv \frac{\partial^2}{\partial z^2}+\frac{\partial^2}{\partial y^2}, \tag{3.6}$$
H is an arbitrary function of ψ (and possibly of $\bar{x}$, which enters only parametrically), and the prime denotes differentiation with respect to ψ.

The solution to this equation must, of course, match with (3.1) at large values of the appropriately scaled spanwise variable and it therefore follows (upon dropping the irrelevant dependence on $\bar{x}$) that
$$\psi \to \pm\frac{\epsilon}{\sigma} y \bar{w}_c(-\sigma \ln y); \quad z \gtrless 0, \tag{3.7}$$
as this variable becomes large. Then ψ will become z-independent and therefore satisfy
$$\partial^2\psi/\partial y^2 \to \tfrac{1}{2}H', \tag{3.8}$$
as the scaled z becomes large. This can easily be integrated to show that
$$y \to \pm\int\frac{\mathrm{d}\psi}{H^{\frac{1}{2}}}; \quad z \gtrless 0. \tag{3.9}$$
Then since y is small (i.e. $-\sigma \ln y = O(1)$) it follows that we must take
$$H = \left[\frac{\epsilon}{\sigma}\bar{w}_c\left(-\sigma \ln\frac{\psi\sigma}{\epsilon}\right)\right]^2 + O(\sigma), \tag{3.10}$$
and therefore that to lowest order in σ
$$\nabla_T^2 \psi = -\frac{\epsilon^2}{\sigma}\frac{\bar{w}_c(-\sigma\ln(\psi\sigma/\epsilon))\,\bar{w}_c'(-\sigma\ln(\psi\sigma/\epsilon))}{\psi}, \tag{3.11}$$
where the prime now denotes differentiation with respect to the indicated argument.

Equation (3.7) suggests that we introduce the new dependent variable $\bar{\psi}$ by
$$\psi = \frac{\epsilon}{\sigma}\mathrm{e}^{-\eta/\sigma}\bar{\psi}. \tag{3.12}$$
Since ψ depends on $\ln y$ the form of the two-dimensional vorticity equation suggests that it will be a function of $\ln z$ so that it is appropriate to take η and
$$\theta = \tfrac{1}{2}\ln(y/z)^2, \tag{3.13}$$
as new independent variables. Then $\bar{\psi}(\bar{x}, \eta, \theta)$ satisfies
$$\sigma\bar{\psi}_{\eta\eta}-\bar{\psi}_\eta-2\bar{\psi}_{\eta\theta}+\frac{1}{\sigma}(1+\mathrm{e}^{2\theta})(\bar{\psi}_{\theta\theta}+\bar{\psi}_\theta) = -\frac{\bar{w}_c(\eta-\sigma\ln\bar{\psi})\,\bar{w}_c'(\eta-\sigma\ln\bar{\psi})}{\bar{\psi}}, \tag{3.14}$$
and the crossflow velocity components v and w are determined by
$$v = \pm\frac{\epsilon}{\sigma}\mathrm{e}^{\theta}\frac{\partial\bar{\psi}}{\partial\theta}; \quad z \gtrless 0, \tag{3.15}$$
and
$$w = \frac{\epsilon}{\sigma}[\bar{\psi}+\bar{\psi}_\theta-\sigma\bar{\psi}_\eta]. \tag{3.16}$$

The matching condition (3.7) requires that

$$\bar{\psi} \to \pm \bar{w}_c(\eta) \quad \text{as} \quad z \to O(1). \tag{3.17}$$

As z moves progressively closer to zero three limiting forms of (3.14) must be considered. The first of these is encountered when

$$0 < \bar{\theta} \equiv -\sigma\theta = O(1). \tag{3.18}$$

In this region, which we denote by region I (see figure 3), (3.14) reduces to

$$\bar{\psi}_{\bar{\theta}} + \bar{\psi}_\eta = \bar{w}_c(\eta)\,\bar{w}_c'(\eta)/\bar{\psi}, \tag{3.19}$$

which is easily solved to obtain

$$\bar{\psi}^2 = G(\eta - \bar{\theta}) + \bar{w}_c^2(\eta), \tag{3.20}$$

where G is an, as yet, arbitrary function of $\eta - \bar{\theta}$. It now follows from (3.15) and (3.16) that

$$v = -\epsilon\, e^{-\bar{\theta}/\sigma} \frac{G'(\eta - \bar{\theta})}{2[G(\eta - \bar{\theta}) + \bar{w}_c^2(\eta)]^{\frac{1}{2}}}, \tag{3.21}$$

$$w = \mp \frac{\epsilon}{\sigma}[G(\eta - \bar{\theta}) + \bar{w}_c^2(\eta)]^{\frac{1}{2}}; \quad z \gtrless 0, \tag{3.22}$$

assuming, as in the numerical example of GLC, that $\bar{w}_c < 0$ for $z > 0$, i.e. that the flow (at infinity) is into the symmetry plane. It is also easy to show, from the spanwise momentum equation, that the pressure, p, is given by

$$p = -\tfrac{1}{2}(\epsilon/\sigma)^2\, G(\eta - \bar{\theta}). \tag{3.23}$$

Since $\bar{\theta} \to 0$ as $z \to 0$ with y (or η) fixed, we can now make $w \to 0$ as $z \to 0$ by choosing

$$G(\eta) \equiv -\bar{w}_c^2(\eta). \tag{3.24}$$

Notice that (2.5), (3.13) and (3.18) show that

$$\eta - \bar{\theta} = -\sigma \ln|z|, \tag{3.25}$$

and (2.12) and (3.2) imply that

$$\bar{w}_c^2 = \sigma\beta_s^3\,\xi_s\,\eta\bar{w}_I^2(\bar{\xi}, 0^+), \tag{3.26}$$

for $\eta < \xi_s/\bar{x}$. It therefore follows that

$$G(\eta - \bar{\theta}) \to \beta_s^3\,\xi_s\,\sigma^2 \ln|z|\,\bar{w}_I^2(\ln|z|, 0^+), \tag{3.27}$$

as $-\sigma\ln|z| \to 0$ and consequently that

$$G(\eta - \bar{\theta}) \to 0 \quad \text{as} \quad -\sigma\ln|z| \to 0, \tag{3.28}$$

which, together with (3.20) shows that the matching condition (3.17) is, in fact, satisfied with this choice of G. However, it follows from (3.21) that v now becomes infinite as $\bar{\theta} \to 0$. In fact (3.20)–(3.24) show that

$$\bar{\psi}^2 \to 2\bar{w}_c(\eta)\,\bar{w}_c'(\eta)\,\bar{\theta}, \tag{3.29}$$

$$v \to \epsilon\, e^{-\bar{\theta}/\sigma}[2\bar{w}_c(\eta)\,\bar{w}_c'(\eta)]^{\frac{1}{2}}/2\bar{\theta}^{\frac{1}{2}}, \tag{3.30}$$

$$w \to \mp\,(\epsilon/\sigma)\,[2\bar{w}_c(\eta)\,\bar{w}_c'(\eta)]^{\frac{1}{2}}\,\bar{\theta}^{\frac{1}{2}}; \quad z \gtrless 0, \tag{3.31}$$

and

$$p \to \tfrac{1}{2}(\epsilon/\sigma)^2\,(\bar{w}_c^2 - 2\bar{w}_c\,\bar{w}_c'\,\bar{\theta}), \tag{3.32}$$

as $\bar{\theta} \to 0$. This means that we have to introduce a new intermediate region closer in toward the symmetry plane.

Since the next significantly different scaling occurs when

$$\theta = O(1), \tag{3.33}$$

we take this to be the appropriate scaling in this region, which we now denote as II (see figure 3). Then it follows from (3.14) and (3.29) that in this region $\bar{\psi}$ will be of the form

$$\bar{\psi} = \sigma^{\frac{1}{2}}(\bar{w}_c \bar{w}_c')^{\frac{1}{2}}\, \Psi(\theta), \tag{3.34}$$

where Ψ is $O(1)$ and satisfies

$$(1+e^{2\theta})(\Psi_{\theta\theta}+\Psi_\theta) = -1/\Psi, \tag{3.35}$$

and it follows from (3.15) and (3.16) that the crossflow velocity components are now given by

$$w = \frac{\epsilon}{\sigma^{\frac{1}{2}}}(\bar{w}_c \bar{w}_c')^{\frac{1}{2}}(\Psi+\Psi_\theta), \tag{3.36}$$

and

$$v = \pm\frac{\epsilon}{\sigma^{\frac{1}{2}}} e^{\theta}(\bar{w}_c \bar{w}_c')^{\frac{1}{2}}\Psi_\theta; \quad z \gtrless 0. \tag{3.37}$$

Matching with (3.29) requires that

$$\Psi \to \mp(-2\theta)^{\frac{1}{2}} \quad \text{as} \quad \theta \to -\infty; \quad z \gtrless 0, \tag{3.38}$$

and since (3.35) reduces to

$$e^{2\theta}(\Psi_{\theta\theta}+\Psi_\theta) = -1/\Psi, \tag{3.39}$$

as $\theta \to +\infty$ it follows that

$$\Psi \to \mp e^{-\theta}(2\theta)^{\frac{1}{2}} \quad \text{as} \quad \theta \to \infty; \quad z \gtrless 0. \tag{3.40}$$

The appropriate signs in (3.40) have been determined by noting that Ψ cannot change sign in $-\infty < \theta < \infty$, that the negative of any solution (3.35) is also a solution, and that θ is an even function of z.

However, (3.37) and (3.40) now show that v still becomes infinite (i.e. it behaves like $\theta^{\frac{1}{2}}$) as $\theta \to \infty$. We therefore have to introduce a third region, say III, that lies even closer to the symmetry plane. The next significantly different scaling occurs when

$$0 < -\bar{\theta} = O(1), \tag{3.41}$$

and matching with (3.34) and (3.40) suggests that the dependent variable will now be of the form

$$\bar{\psi} = e^{\bar{\theta}/\sigma}\hat{\Psi}(\eta, \bar{\theta}), \tag{3.42}$$

and that $\hat{\Psi}$ will then be $O(1)$ and satisfy the matching condition

$$\hat{\Psi} \to \mp(2\bar{w}_c \bar{w}_c')^{\frac{1}{2}}(-\bar{\theta})^{\frac{1}{2}} \quad \text{as} \quad \bar{\theta} \to 0; \quad z \gtrless 0. \tag{3.43}$$

Substituting the new variables (3.41) and (3.42) into (3.14) shows that $\hat{\Psi}$ is determined by

$$\hat{\Psi}\,\partial\hat{\Psi}/\partial\bar{\theta} = -\bar{w}_c(\eta-\bar{\theta})\,\bar{w}_c'(\eta-\bar{\theta}), \tag{3.44}$$

and it follows from (3.15) and (3.16) that the crossflow velocity components are now given by

$$v = \mp\frac{\epsilon}{\sigma}\hat{\Psi}; \quad z \gtrless 0, \tag{3.45}$$

$$w = -\epsilon\, e^{\bar{\theta}/\sigma}[\hat{\Psi}_{\bar{\theta}}+\hat{\Psi}_\eta]. \tag{3.46}$$

The solution to (3.44) that satisfies the matching condition (3.43) is given by

$$\hat{\Psi} = \mp [\bar{w}_c^2(\eta - \bar{\theta}) - \bar{w}_c^2(\eta)]^{\frac{1}{2}}; \quad z \gtrless 0. \tag{3.47}$$

Then (3.45) and (3.46) show that the crossflow velocity components now both remain bounded as $\bar{\theta} \to -\infty$, and consequently as $z \to 0$, and since (3.13) and (3.18) show that

$$e^{\bar{\theta}/\sigma} = |z|/y, \tag{3.48}$$

they are both also continuous there.

4. Discussion

We have now shown that a completely smooth inviscid solution can be found for the blending-layer, or nonlinear vorticity-layer, region by piecing together appropriate local solutions. In the main part of the flow the crossflow velocity is determined by the inviscid Burgers' equation independently of the other velocity components, i.e. it is decoupled from the other velocity components, and the horizontal pressure gradients are negligible. The infinite singularity in the vertical velocity that resulted from the initial breakdown of the inviscid Burgers' equation solution was eliminated by the singularity line solution in GLC. The spanwise and vertical velocities were fully coupled but the horizontal pressure gradients were still negligible in this solution. This left the finite discontinuities in the spanwise velocity which are completely eliminated in the present paper. First, there is an outer region, referred to as I in figure 3, in which the flow perturbation is primarily in the spanwise direction and predominantly one-dimensional. In this region, where $\eta = O(1)$ and $|z| \gg y$ or, more precisely, $-\sigma \ln |z| < \eta \equiv -\sigma \ln y$, a strong adverse pressure gradient is set up in the spanwise direction to reduce the spanwise velocity to zero and thereby eliminate the spanwise velocity discontinuity. We computed the scaled pressure in region I from (3.2), (3.23), (3.24), (3.26) and the solutions for $\bar{w}_0$ and $\bar{w}_1$ given in GLC. Numerical values had to be specified for the parameters σ, ξ_Δ, ξ_s and $\bar{x}$ appearing in these solutions. These were chosen, as far as possible, to correspond to the numerical example of GLC. The result is plotted in figure 4 and the parameter values are given in the caption. Figure 4 shows that the pressure increases monotonically from zero as the flow penetrates region I. This caused the vertical velocity to become unbounded as the symmetry plane was approached and a new inner scaling had to be introduced corresponding to region II in figure 3.

The region I vertical velocity is exponentially small compared with the spanwise velocity while the reverse is true in region III. In fact the velocity components in these regions are related by

$$v^{\mathrm{I}}(\eta, \bar{\theta}) = \mp\, w^{\mathrm{III}}(\eta - \bar{\theta}, -\bar{\theta}), \tag{4.1}$$

$$w^{\mathrm{I}}(\eta, \bar{\theta}) = \mp\, v^{\mathrm{III}}(\eta - \bar{\theta}, -\bar{\theta}), \tag{4.2}$$

where the superscripts refer to the solutions in regions I and III. The (y, z)-plane streamlines are therefore essentially horizontal and vertical straight lines within regions I and III, respectively so there is no need to present them graphically. However, the spanwise and vertical velocities are of the same order in region II, where $\eta = O(1)$ and $z = O(y)$, and the flow is turned from the spanwise direction to the vertical. To show this turning we numerically solved (3.35), subject to the boundary conditions (3.38) and (3.40), and combined the results with (3.34) and (3.14) to obtain $\sigma\psi/\epsilon$ as a function of y and z. The values for the parameters are the

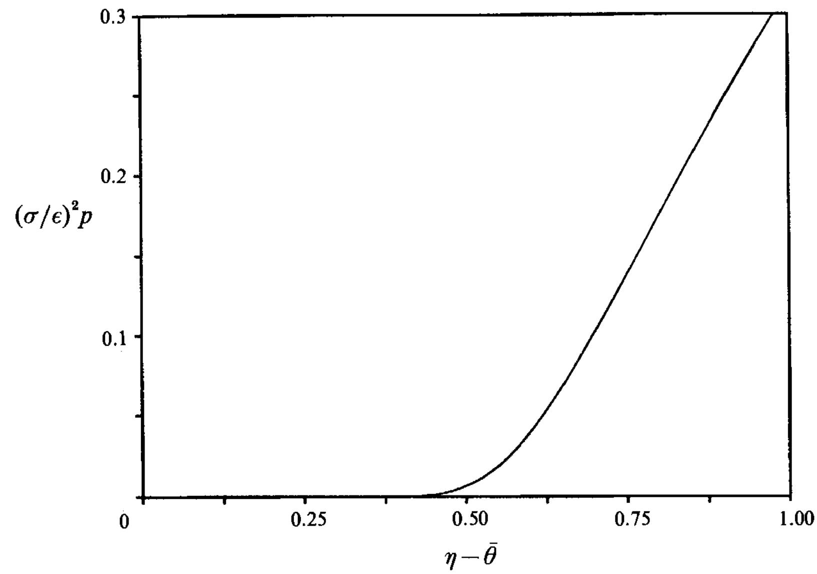

FIGURE 4. Variation of the scaled pressure in region I. Computed with parameter values chosen as $\sigma = 0.1$, $\xi_\Delta = \frac{1}{4}$, $\xi_s = 1$, $\bar{x} = 2$.

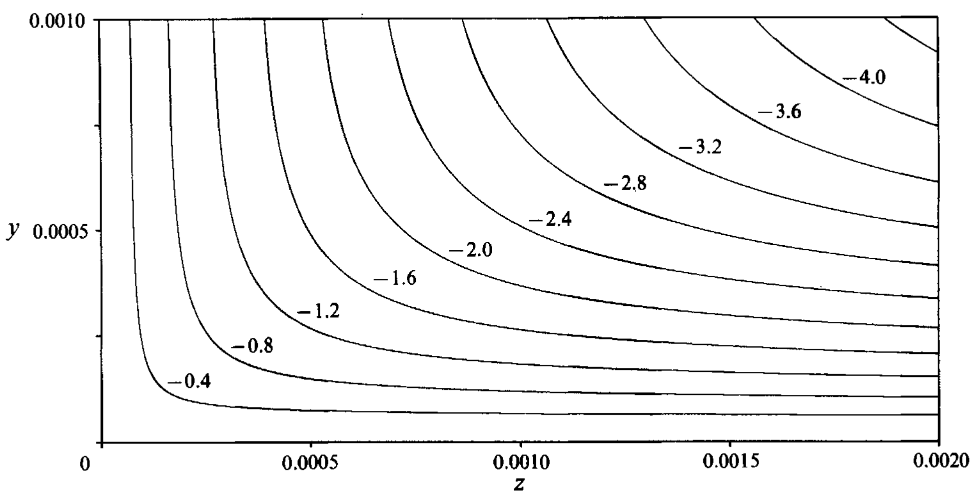

FIGURE 5. Contours of $(\sigma/\epsilon)\,\psi \times 10^4$ in region II. Same parameter values as in figure 4.

same as those used to compute the pressure in figure 4. The contours of this scaled streamfunction are plotted in figure 5. This streamline pattern clearly shows that the flow is turned from the spanwise to the vertical direction. The turning is, however, incomplete and, as a result, the vertical velocity develops another singularity closer in toward the symmetry plane. This singularity is eliminated by introducing a third asymptotic region in which $\eta = O(1)$ and $|z| \ll y$ (or $-\sigma \ln |z| > \eta$). This is referred to as region III in figure 3. Here the vertical velocity become large and the flow has a vertical jet-like structure.

Since the inviscid flow solution is completely non-singular, any singularity in the problem would arise due to a breakdown of the viscous boundary-layer flow. In fact, while this flow structure is acceptable from a purely inviscid point of view, it will not always be realizable in practice because the strong spanwise deceleration of the flow in region I will usually separate the boundary layer at the surface of the plate if that layer remains laminar (see also the discussion at the end of GLC).

The authors would like to thank Professor A. F. Messiter for helpful discussions and for pointing out the relations (4.1) and (4.2).

REFERENCES

GOLDSTEIN, M. E. 1978 Unsteady vortical and entropic distortions of potential flows round arbitrary obstacles. *J. Fluid Mech.* **89**, 433–468.

GOLDSTEIN, M. E., LEIB, S. J. & COWLEY, S. J. 1992 Distortion of a flat plate boundary layer by free stream vorticity normal to the plate. *J. Fluid Mech.* **237**, 231–260 (referred to herein as GLC).

HUNT, J. C. R. & CARRUTHERS, D. J. 1990 Rapid distortion theory and the 'problems' of turbulence. *J. Fluid Mech.* **212**, 497–532.

LIGHTHILL, M. J. 1956 Drift. *J. Fluid Mech.* **1**, 31–53.

STEWARTSON, K., CEBECI, T. & CHANG, K. C. 1980 A boundary layer collision in a curved duct. *Q. J. Mech. Appl. Maths* **33**, 59–75.

STEWARTSON, K. & SIMPSON, C. J. 1982 On a singularity initiating a boundary layer collision. *Q. J. Mech. Appl. Maths* **35**, 1–16.